Regulation of Fibronectin Receptor Distribution by Transformation, Exogenous Fibronectin, and Synthetic Peptides

Wen-Tien Chen,* Jie Wang,* Takayuki Hasegawa,*‡ Susan S. Yamada,‡ and Kenneth M. Yamada‡

*Department of Anatomy and Cell Biology, Georgetown University Medical Center, Washington, D.C. 20007;
‡Laboratory of Molecular Biology, National Cancer Institute, Bethesda, Maryland 20892

Abstract. Recent studies have shown that fibronectin and its 140K membrane receptor complex are spatially associated with microfilaments to form cell surface linkage complexes which are thought to mediate adhesive interactions between fibroblasts and their substrata. We examined the regulation of the organization of these cell surface structures in transformed and fibronectin-reconstituted cells as well as in cells treated with a competitive synthetic peptide inhibitor of fibronectin binding to its receptor. Correlative localization experiments with interference reflection microscopy and double-label or triple-label immunofluorescence revealed a concomitant loss of fibronectin, 140K receptor, and alpha-actinin colocalization at cell substratum extracellular matrix contact sites after transformation of chick fibroblasts by wild-type or temperature-sensitive Rous sarcoma viruses (RSV). Western and dot immunoblot analyses established that although similar total quantities of intact 140K molecules were present in the transformed cell cultures, significantly more was released into the culture medium of transformed cells. The 140K molecules on transformed cells were available for interaction with exogenously added fibronectin, which could reconstitute fibronectin–140K linkage complexes. In such fibronectin reconstitution experiments, many cells expressed both fibronectin–140K–actin linkage complexes and RSV pp60^{src}, indicating that the morphological reversion could occur even in the continued presence of RSV transformation. The synthetic peptide Gly-Arg-Gly-Asp-Ser derived from the sequence of the cell-binding region of fibronectin could also prevent the organization of fibronectin–140K linkage complexes. Our results suggest that fibronectin interaction with cells regulates the organization of fibronectin receptor complexes and cytoskeletal components at the cell surface.

ADHESIVE interactions of cells with the extracellular matrix (ECM)[1] are critically important events for morphogenetic movements during embryonic development and for cancer cell invasion during metastasis (34, 36, 41). These processes could be guided by temporal and spatial changes in the composition of cell adhesion molecules and receptors in the plasma membrane that interact with other cells or with ECM molecules (36). Fibronectin is a major extracellular glycoprotein that is implicated in the adhesion and spreading of fibroblastic cells (see references 26, 28, 34, and 41 for reviews). Fibronectin-mediated cell adhesion and spreading occur at discrete membrane regions in cultured cells and appear to be mediated by integral membrane receptors for fibronectin (1, 6, 10, 11, 19, 20, 24, 29, 32). In several types of avian cells, a complex of glycoproteins averaging 140,000 in apparent molecular weight on SDS polyacrylamide gels (referred to here as the 140K complex) has recently been shown to be involved in the binding of cells to fibronectin by in situ localization studies (10, 11, 14, 16), immunological inhibition studies (5, 6, 10, 14, 16, 19, 29), and by its direct binding to fibronectin (1, 24, 32). Based on the morphological finding that 140K molecules colocalize with both fibronectin and microfilament bundles (10, 11, 14, 16, 33), it was proposed that the 140K fibronectin receptor complex may be part of a cell surface linkage between fibronectin and cytoskeleton, which anchors cells to their substrata and maintains normal morphology.

Oncogenic transformation of cultured cells by viruses causes a pleiotropic change in cellular properties, including the classical observations of reduced adhesion (38) and rounded morphology (15, 39). Explanations for this phenomena include increased production of cell surface proteases (12, 17), and loss of fibronectin (21, 22, 25, 30), cytoskeletal organization (15, 35, 39), or cell–cell adhesion molecules (4). Since many of these changes can be reverted to some extent by the addition of fibronectin (2, 39, 44), it has been suggested that loss of fibronectin may be important for producing the transformed phenotype and may be associated with detachment and subsequent invasion of malignant cells in vivo (e.g., see references 12, 15, and 34). It is not known, however, whether the expression or organization of 140K molecules is affected by cellular transformation. More

1. *Abbreviations used in this paper*: CEF, chicken embryonic fibroblasts; ECM, extracellular matrix; GRGDS, Gly-Arg-Gly-Asp-Ser; IRM, interference reflection microscopy; RSV, Rous sarcoma virus; RSV-CEF, chicken embryonic fibroblasts transformed by Rous sarcoma virus.

generally, it is not known how the quantities or distribution of this recently discovered receptor complex are regulated.

In this paper, we address the following questions: (*a*) Does transformation change the expression of 140K receptor molecules on the cell surface? (*b*) How are cell surface linkage complexes altered in transformed cells? and (*c*) Does fibronectin play a regulatory role in the organization of cell surface linkages? To attempt to answer these questions, we analyzed the expression and distribution of the 140K complex on the cell surface of Rous sarcoma virus (RSV)–transformed cells, the effects of exogenous fibronectin on the organization of cell surface 140K molecules, and the effects of inhibiting fibronectin binding to the cell surface by the synthetic peptide Gly-Arg-Gly-Asp-Ser (GRGDS) derived from the sequence of the cell-binding region of fibronectin. Part of this work has been presented in abstract form (37).

Materials and Methods

Cell Culture

Chicken embryonic fibroblasts (CEF) and CEF cells transformed by the wild-type Schmidt-Ruppin strain of RSV (RSV-CEF) or the ts68 (tsNY68) temperature-sensitive mutant of RSV (a gift from Drs. S. Kawai and H. Hanafusa, The Rockefeller University) were obtained and cultured as described (12, 30) in Dulbecco's modified Eagle's medium containing 4,500 mg/liter of glucose, 10% fetal calf serum, 10 μg/ml gentamycin, and 2 mM glutamine. Cells were seeded on coverslips at an initial density of 5×10^4 cells per 35-mm diam tissue culture dish and cultured for 18 h before fixation for immunofluorescence or performance of inhibition assays with antibodies or synthetic peptides.

Antibody Reagents

Mouse JG22E monoclonal antibody and rabbit polyclonal antibody directed against the 140K complex (10), mouse EB7 monoclonal antibody directed against the $pp60^{src}$ oncogene product of RSV (9, 31), rabbit anti-fibronectin antibody (10, 12), fluoresceinated goat anti-fibronectin antibody (40), and affinity-purified rabbit anti-vinculin and rabbit anti-alpha-actinin antibodies (13) were prepared and characterized as described. Rhodamine-conjugated goat antibodies to mouse IgG and fluorescein-conjugated goat antibodies to rabbit IgG were affinity purified on the relevant antigen immunoabsorbent prepared using Ultrogel AcA-22 (LKB Instruments, Inc., Gaithersburg, MD). Rhodamine conjugates of affinity-purified goat antibody (Fab′ fragments) against rabbit IgG were purchased from Cooper Biomedical, Inc. (Malvern, PA). Cross-reactivity among these antibody reagents was negligible (10).

Correlative Localization by Interference Reflection Microscopy (IRM) and Indirect Double- or Triple-label Immunofluorescence

Cells cultured on 22 × 22-mm glass coverslips for 18 h were fixed with 3% paraformaldehyde, permeabilized with 0.4% Triton X-100, and double- or triple-immunolabeled according to the labeling procedure described previously (10, 13). Each antibody was applied at a concentration of 10 μg/ml. Several types of specificity control experiments were performed as described (10), and the controls showed negligible labeling. For triple-label experiments, three fields of double-immunolabeled cells were photographed for each coverslip, photobleached to destroy the fluorescein fluorochrome, labeled with the third antibody (fluorescein conjugates of goat anti-fibronectin antibody) in the filming chamber, and the cells were relocated on the microscope stage for photography of the third labeling step (10). Cross-reactivity among the antibody reagents used in the triple-label experiment was negligible, and there was no fluorescein fluorescence visible when cells were examined after the photobleaching step and before addition of the third label. Labeled cells were photographed with an Antiflex-Neofluar 63/1.25 objective (Carl Zeiss, Inc., Thornwood, NY) on a Zeiss Photomicroscope III by IRM then by epifluorescence microscopy for rhodamine and fluorescein labeling.

Quantitative Immunofluorescence

Measurements of relative fluorescence intensity on individual cells in CEF and RSV-CEF cultures were performed by using the spot measurement system of the Zeiss Photomicroscope III. Using the Planapo 63/1.4 objective, the plane of focus was set at the cell-substratum interface, and specific areas of the ventral cell surface, i.e., ECM contacts in normal cells and rosette contacts in transformed cells, were placed in the circle in the center of the reticle field. Measurements were made by closing the field diaphragm to establish an illumination field 3 μm in diameter, setting the automatic exposure dial to ASA 6400, and recording the length of time in seconds required to reach 50% exposure. Measurements were expressed in arbitrary units by defining the intensity of anti-140K JG22E monoclonal antibody staining on the ventral cell surface of normal CEF cells containing ECM contacts as ten units, and that of control myeloma IgG staining of the same region as one unit. The method takes advantage of the narrow depth of field of the Planapo 63/1.4 objective to measure only a narrow optical section at the plane of cell-substratum contact, and the small field window of 3 μm permits measurements of specific local areas of the cell membrane; the method thus estimates the relative amount of antigen per unit cell membrane.

Quantitation of the 140K Complex in Cell Cultures

The amounts of 140K complex in the media and whole-cell homogenates of CEF and RSV-CEF cultures were quantitated by dot immunoblot (1, 27) and Western immunoblot analyses (7, 10) using rabbit polyclonal antibodies directed against the chick 140K complex. In each experiment, 5×10^5 or 10^6 cells were plated in 35-mm dishes in 2 ml of medium, or 1.8×10^7 cells were plated in 100-mm dishes in 10 ml of medium, then fed at day 1. Culture media were collected at the end of day 2 (24 h after feeding), centrifuged to remove floating cells, adjusted to 2% SDS by the addition of one-quarter volume 10% SDS, and assayed for released 140K complex. Controls for the released 140K antigen included media incubated in parallel without cells to quantitate any nonspecific labeling. After 2 d in culture, the cell layers were washed with phosphate-buffered saline (PBS) and then solubilized in 0.5 ml 2% SDS in 10 mM sodium phosphate, pH 7.0, containing 2 mM phenylmethylsulfonyl fluoride (Sigma Chemical Co., St. Louis, MO) by scraping, vortex agitation, and heating to 100°C for 3 min.

To quantitate the 140K complex in CEF and RSV-CEF cultures, SDS-containing media or SDS homogenates of CEF or RSV-CEF cell layers were analyzed by dot immunoblot analysis exactly as described previously (1) using standards of purified 140K complex obtained by JG22E-immunoaffinity chromatography (20). 3-μl aliquots were spotted in the center of 1 × 1-cm grids drawn on nitrocellulose filter paper (0.45-μm pore size, type BA85; Schleicher & Schuell, Inc., Keene, NH). The dotted nitrocellulose sheets were blocked with 5% bovine serum albumin (BSA), then incubated with a 1/200 dilution of polyclonal rabbit antibody to 140K antigen for 90 min, rinsed extensively, then incubated with 5×10^5 cpm/ml ^{125}I-labeled protein A (New England Nuclear, Boston, MA). After rinsing and drying, the blots were visualized by autoradiography with Kodak X-Omat film or quantitated by excising each square in the grid and determining radioactivity in an LKB-Wallac 1275 Mini-gamma counter as described (1).

Proteins in aliquots of SDS homogenates of CEF or RSV-CEF cell layers were electrophoretically resolved under nonreducing conditions by SDS polyacrylamide slab gel electrophoresis using 4% stacking and 7.5% resolving gels, and then Western immunoblotting was performed as described (7)

Figure 1. Distribution of 140K receptor (*140K*), alpha-actinin (*A*), and fibronectin (*FN*) in a normal CEF (*left*) and in a CEF infected with wild-type RSV (*right*) grown at 37°C. The cells were immunofluorescently triple-labeled for 140K, A, and FN and observed by IRM. Filled arrows (*left*) point to the same ECM contact sites in a normal CEF and indicate cell surface linkage complexes at the cell–substratum interface which are visualized as fine IRM streaks and are labeled positively for 140K, A, and FN. Arrowheads (*right*) point to the same rosette contact sites in the same transformed CEF cell, which are visualized as IRM spots and labeled positively for A and only diffusely for 140K, but negatively for FN. Open arrows point to identical focal adhesion sites in IRM of normal (*left*) and transformed CEF (*right*), respectively. Bar, 10 μm.

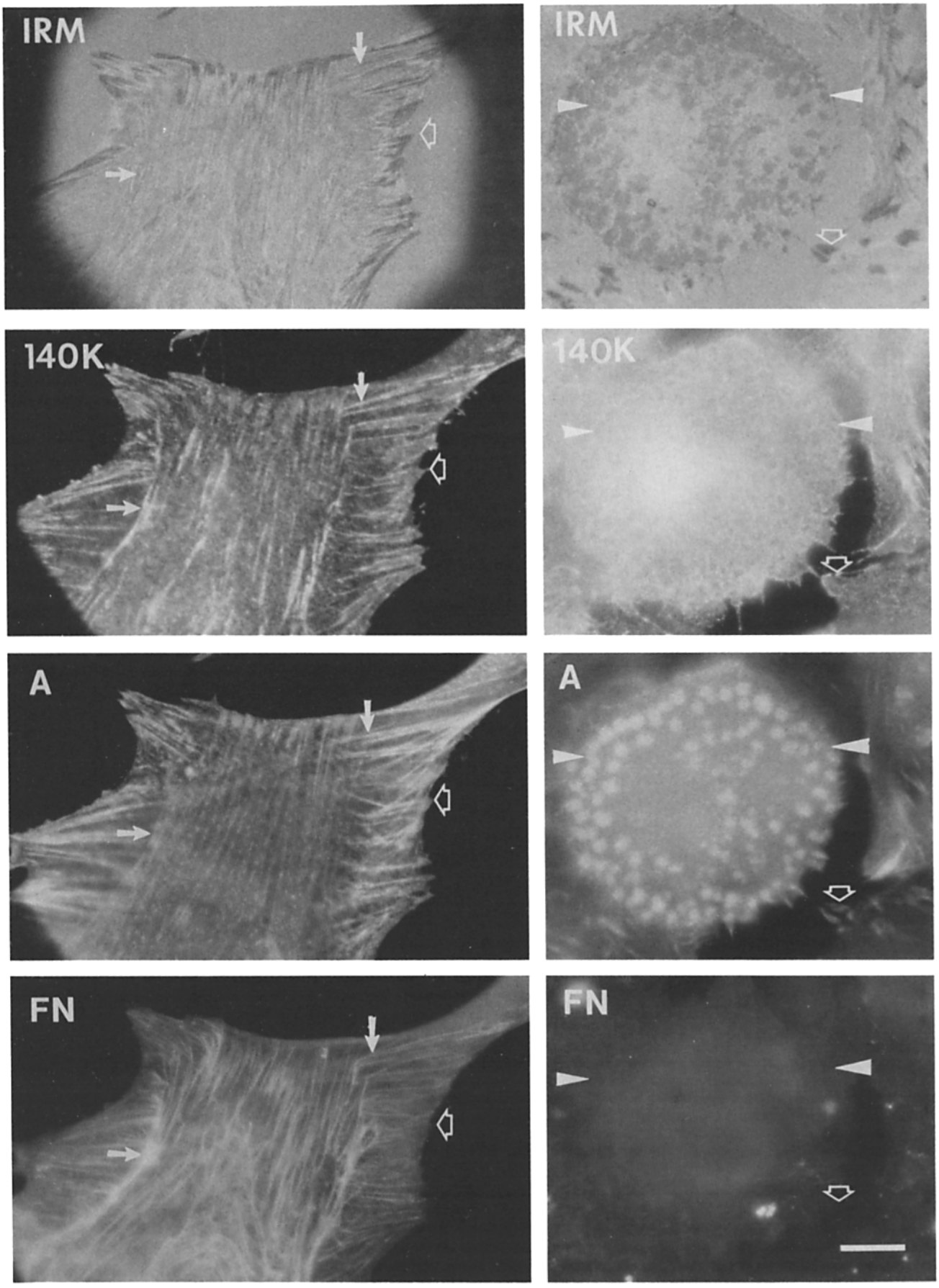
IRM
IRM
140K
140K
A
A
FN
FN

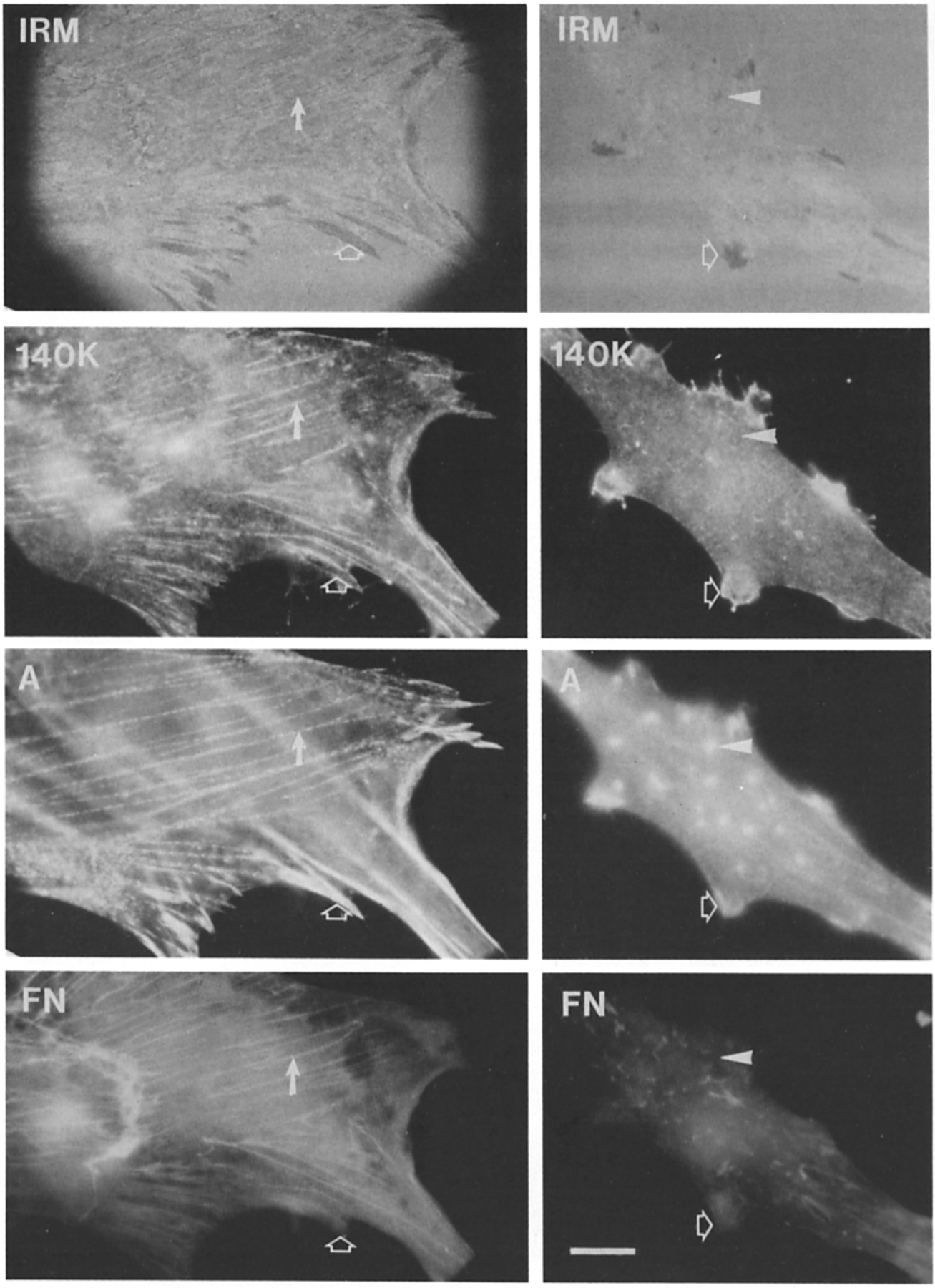
IRM
IRM
140K
140K
A
A
FN
FN

using a borate transfer buffer without SDS (10) in a Trans-blot apparatus (Bio-Rad Laboratories, Richmond, CA) for 2 h at 4°C. Immunoreactivity of anti-140K antibodies with polypeptides in the SDS extracts was visualized after incubating the blots with 5% BSA overnight, staining with rabbit anti-140K antibody and then with ^{125}I-protein A as previously described (7, 10). The antibodies reacted primarily against band 3 (M_r 120,000) of the 140K complex, although some antibodies also bound to band 1 and 2 (M_r 155,000 and M_r 135,000, respectively) in low amounts (see Fig. 4 *B*).

Interaction of Exogenous Fibronectin with the Cell Surface

Cellular fibronectin was obtained from confluent CEF cultures extracted with 1 M urea and 2 mM phenylmethylsulfonyl fluoride and purified as described (40). To reconstitute fibronectin on the cell surface of transformed cells, chicken cellular fibronectin was added to the cell suspension of RSV-CEF at a final concentration of 50 μg/ml during subculturing. We examined the effects of added cellular fibronectin by IRM and immunofluorescence after culturing for 6 h.

Synthetic Peptides

The synthetic peptide GRGDS derived from the cell-binding domain of fibronectin was synthesized to our specifications by Peninsula Laboratories, Inc. (Belmont, CA) and was purified by reverse-phase high-performance liquid chromatography on a preparative C18 column and characterized as described (42, 43). Assays for inhibition of cell adhesion by the GRGDS peptide were performed as described previously (42, 43). We studied the detaching effect of the peptide on third-passage CEF and RSV-CEF that had been in culture for 18 h. The culture medium was removed and replaced with the same serum-containing medium plus 200 μg/ml of the GRGDS peptide. The cells were fixed 10, 20, and 30 min after the addition of the peptide; after 30 min of peptide treatment, >95% of the cells were rounded or detached. No detachment was observed with a closely related peptide (Gly-Arg-Gly-Asp at 200 μg/ml).

Results

Loss of Colocalization of Fibronectin, 140K Receptor, and Alpha-Actinin on the Transformed Cell Surface

Normal fibroblasts contain cell surface linkage complexes with colinear distributions of 140K fibronectin receptor, extracellular fibronectin, and intracellular alpha-actinin (Fig. 1 and reference 10). As visualized by a combination of IRM and triple-immunolabeling techniques, most 140K labeling in CEF was characteristically concentrated in linkage complexes consisting of fibronectin and alpha-actinin (Fig. 1, *left*), superimposed on a weaker, diffuse pattern of 140K labeling. These linkage complexes are visualized by IRM as "ECM contacts" at cell-substratum interfaces (10), and are characterized by their fine, streak-like positive- or negative-contrast images in IRM (Fig. 1, arrows).

CEF infected by the wild-type Schmidt-Ruppin strain of RSV showed a dramatic loss of these cell surface linkage complexes (Fig. 1, *right*). Concomitant with the known loss of fibronectin (12, 30, 40), there was a redistribution of the 140K receptor antigen from alpha-actinin–140K–fibronectin linkages to a diffuse organization on the membrane of transformed cells, and of alpha-actinin from microfilament bundles to patches (Fig. 1, *right*). In place of the normal streak-like ECM contacts seen by IRM on the ventral cell surface, the transformed cells displayed mottled spots detected by IRM, termed "rosette" contacts (15), that were labeled strongly for alpha-actinin, weakly for 140K, and were not labeled for fibronectin. Rosette contacts consist of sets of IRM-dark patches or spots on planar substrata and are predominantly localized under the center of RSV-transformed cells (Figs. 1–3, 5, and 6; see also references 9, 12, 15, and 18); the rosettes are rich in RSV pp60^{src}, alpha-actinin, vinculin, and actin (Figs. 1–3, 5, and 6). The area and organization of the rosettes varied from cell to cell: the predominant pattern of dispersed rosettes, as shown in Fig. 2, was found in 78% of the transformed cells; the compact rosette pattern shown in Fig. 1 represented a minor fraction (22%). However, in rare cases (<3% of the total), we observed concentrations of the 140K antigen immediately surrounding the rosette, coinciding with vinculin localization (Fig. 3). This unusual colocalization of 140K and vinculin may represent a transitional form during dynamic alterations of membrane–cytoskeletal interactions during transformation, as it is less evident in the more compact rosettes characteristic of most transformed cells (Figs. 1 and 2).

These alterations in cell surface linkage complexes were apparently associated with transformation itself, rather than simply with viral infection, since similar results were obtained with CEF infected by the ts68 temperature-sensitive mutant of RSV grown at temperatures nonpermissive or permissive for expression of the transformed phenotype. At the temperature nonpermissive for transformation (41°C), the ts68-infected CEF appeared similar by IRM and immunofluorescence to normal uninfected cells (compare left panels of Figs. 1 and 2). In contrast, cells grown at the temperature permissive for transformation (37°C) were less well spread, lost ECM contacts, and displayed a relatively diffuse pattern of 140K antigen labeling (Fig. 2, *right*). As also found with wild-type RSV, alpha-actinin labeling shifted from the normal pattern of linear streaks to patches often associated with rosettes. Controls included performing the same temperature-shift experiments with uninfected cells or cells transformed by wild-type virus, which showed no alterations in IRM or immunofluorescence patterns.

Expression of the 140K Complex by RSV-CEF and Its Release from Cells

The expression of the 140K antigen in CEF and RSV-CEF cultures was analyzed by several methods. The amounts and distribution of 140K on the surfaces of normal and transformed cells was visualized by indirect immunofluorescent staining using JG22E monoclonal antibody as shown in Figs. 1–3. For semi-quantitative comparisons of the local content

Figure 2. Distribution of 140K fibronectin receptor (*140K*), alpha-actinin (*A*), and fibronectin (*FN*) in temperature-sensitive mutant ts68-infected CEF grown at the nonpermissive temperature (41°C) (*left*) and at the temperature (37°C) permissive for transformation (*right*). The cells were immunofluorescently triple-labeled for 140K, A, and FN, and observed by IRM. Filled arrows (*left*) point to the same ECM contact site in the same infected CEF cell, which displays a normal phenotypic morphology (nonpermissive temperature). The ECM contacts are seen as fine IRM streaks and are labeled positively for 140K, A, and FN. Arrowheads (*right*) point to the same rosette contact site in an infected CEF cell displaying the transformed phenotypic morphology (permissive temperature) showing disrupted linkages; the rosettes are visualized as IRM spots labeled strongly for A and only diffusely for 140K, as well as negatively for FN. Open arrows (*left* and *right*) point to identical focal adhesion sites in IRM of normal and transformed CEF, respectively, where 140K and FN appear to surround, but not convincingly enter, these A-positive focal adhesion sites. Bar, 10 μm.

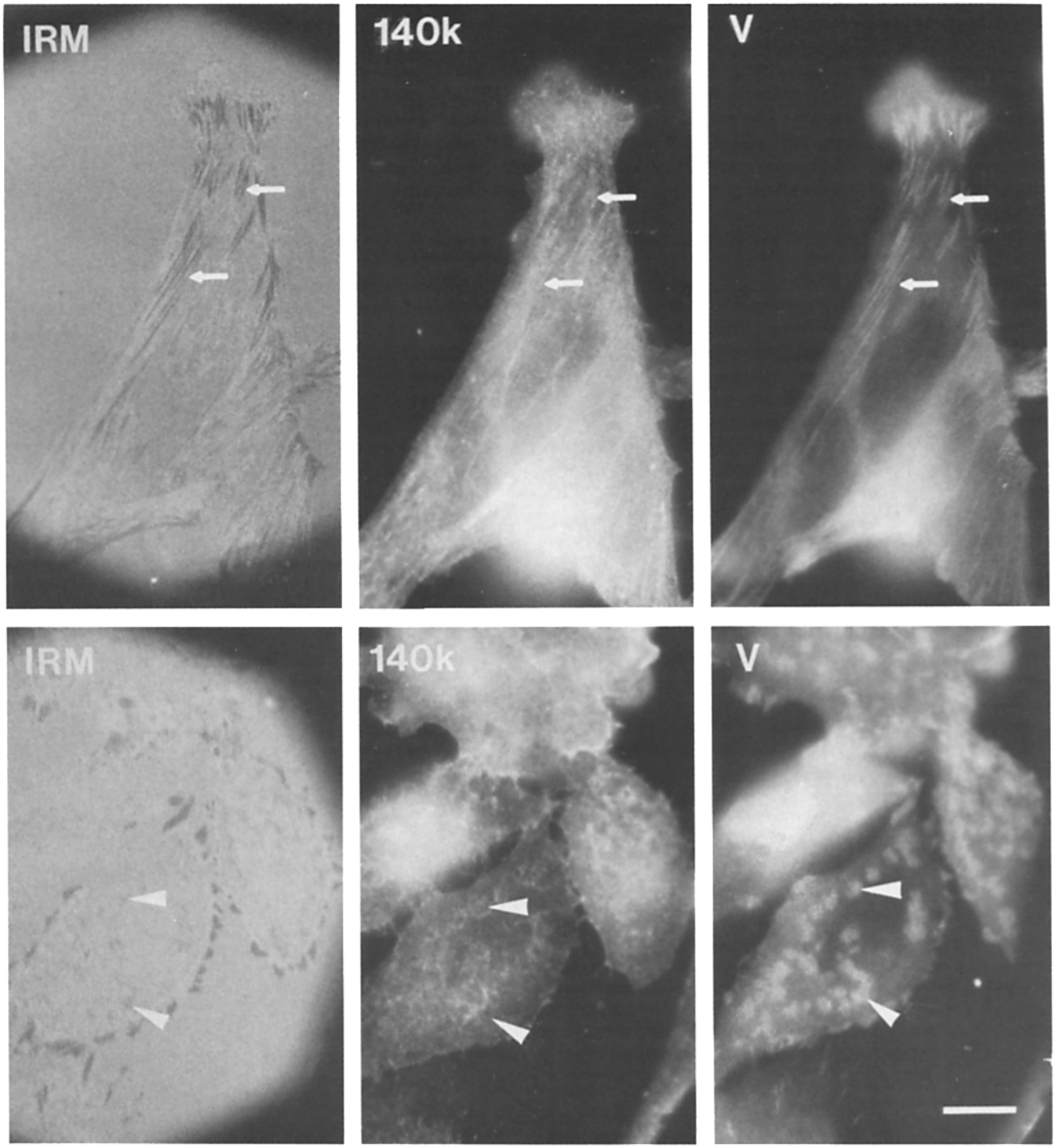

Figure 3. Distribution of 140K antigen (*140K*) and vinculin (*V*) in normal CEF (*top*) and RSV-CEF (*bottom*). The cells were doubly immunofluorescently labeled for 140K and V, and observed by IRM. Arrows indicate ECM contact sites that show concentration of both 140K and V by double labeling. Arrowheads point to rosette contacts in transformed cells which are rich in V, but in which higher concentrations of 140K appear to surround the rosette sites. Bar, 10 μm.

of 140K molecules in CEF and RSV-CEF, we analyzed immunofluorescent intensities in ECM contacts of normal cells and in the corresponding rosette contacts of transformed cells by photomicroscopic measurements of immunofluorescence (see Materials and Methods). Table II shows the results of these experiments. The 140K antigen showed the brightest intensities in the ECM contacts of CEF (12 units) and of ts68-infected CEF grown at the temperature (41°C) nonpermissive for transformation (10 units), which was generally brighter than the rosette contacts of RSV-CEF (8 units). Control myeloma IgG showed very low levels of nonspecific staining (1 unit). These morphologically transformed cells exhibited not only increased levels of 140K staining, but also high levels of RSV pp60^{src} labeling (Table II).

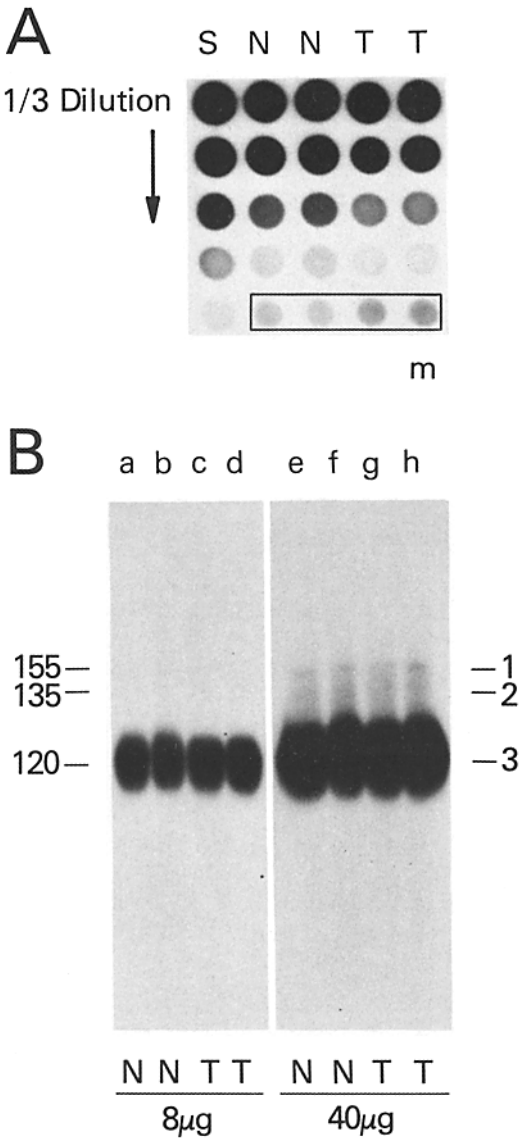

Figure 4. Quantitation of the 140K receptor antigen in CEF and RSV-CEF cultures using rabbit anti-140K antibodies in dot blot (*A*) and Western blot (*B*) analyses. (*A*) Dot immunoblotting of SDS extracts of cell layers and media (*m*) from normal CEF (*N*) and from transformed RSV-CEF (*T*) cultures using as standards (*S*) purified 140K antigen obtained by JG22E-immunoaffinity chromatography. Samples were prepared as described in Materials and Methods, and each sample was spotted in a volume of 3 μl. The upper four rows are serial one-third dilutions of standard (*S*), and cell extracts from CEF (*N*) and from RSV-CEF (*T*), while the boxed samples in the bottom row are four undiluted, independent samples of medium (*m*). Concentrations of the JG22E-purified 140K antigen started with 50 ng/3 μl of antigen in the vertical row of standards (*S*) and also represent serial one-third dilutions from top to bottom. In this experiment, cell extracts from normal cells (*N*) contain slightly more 140K antigen than transformed cell extracts (*T*), particularly noticeable in the third and fourth horizontal rows. However, the T medium spots contain significantly more 140K antigen (~1.4 ng) than the N medium spots (~1.1 ng), as shown in the bottom row. (*B*) The amounts and molecular forms of 140K antigens that were specifically identified in whole-cell SDS homogenates from duplicate transformed cell cultures (*T*) (lanes *c*, *d*, *g*, and *h*) and from duplicate normal cultures (*N*) (lanes *a*, *b*, *e*, and *f*) according to Western immunoblot analysis in an SDS polyacrylamide slab gel with 4% stacking and 7.5% resolving gels. Lanes *a–d* each contain 8 μg of sample, while lanes *e–h* contain 40 μg of sample. Apparent molecular weights are indicated on the left and band designations on the right.

The type and content of 140K antigens expressed by the normal and transformed CEF were further examined using rabbit polyclonal anti-140K antibodies in Western and dot immunoblot analyses (see Fig. 4 and Materials and Methods). CEF and RSV-CEF that had been cultured for 2 d were homogenized in SDS, and the whole-cell SDS extracts were analyzed on Western blots (Fig. 4 *B*). The anti-140K antibodies bound mostly to the 120,000-D band 3, of the three-component JG22E antigen of normal cells (Fig. 4 *B*, lanes *a*, *b*, *e*, and *f*, and references 10 and 20) and of cells transformed by RSV (Fig. 4 *B*, lanes *c*, *d*, *g*, and *h*). A small amount of anti-140K antibody bound to the higher molecular weight components of the JG22E antigen (bands *1* and *2*) in all fractionated extracts (Fig. 4 *B* and references 10 and 20). In all experiments, the immunoblotting patterns of 140K complexes from normal and transformed CEF were indistinguishable from each other, suggesting that 140K receptor complex exists in similar molecular forms in both CEF and RSV-CEF. However, densitometric scanning of the autoradiograph revealed that the normal cell extract contained ~8% more 140K antigen than the transformed cell extract (Fig. 4 *B*).

We verified this possible difference in 140K protein content by dot immunoblotting of SDS extracts and culture media from normal and transformed CEF using as standards purified 140K complex obtained by JG22E-immunoaffinity chromatography (Fig. 4 *A* and Table I). The sum of the quantities of 140K antigen in cell layers and media showed only minimal differences between total 140K production in normal and transformed cells (e.g., 4–10% in the experiment shown in Table I). However, in all experiments, the media of RSV-CEF contained substantially more released 140K antigen than those of RSV-CEF (e.g., 40–60% more in the experiment quantitated in Table I).

Reconstitution of Fibronectin–140K Linkage Complexes in Transformed Cells

Culturing of RSV-infected CEF in the presence of added cellular fibronectin caused changes in the morphology of these cells toward that of normal cells and restored a cell surface matrix of fibronectin, as previously shown in avian and mammalian cells (2, 40, 44). However, primary cultures of RSV-transformed cells can contain a small subpopulation of untransformed cells (see also reference 4), which are difficult to distinguish from fibronectin-reconstituted transformed cells because their morphologies are so similar. To ensure that all of the fibronectin-reconstituted cells we examined were derived from RSV-transformed cells, RSV-infected CEF cultures were double-immunofluorescently labeled with the mouse EB7 monoclonal antibody directed against RSV pp60^{src} and goat anti-fibronectin antibodies (Fig. 5). Transformed cells expressed RSV pp60^{src} specifically localized to the "rosette" contacts, which contained alpha-actinin but were found to lack cell surface-associated fibronectin (Fig. 5, *A* and *B*). In cells treated with added cellular fibronectin, the total area of RSV pp60^{src}-positive rosettes was reduced, and they became localized under the center of the cells; concomitantly, new cell surface-associated fibronectin appeared

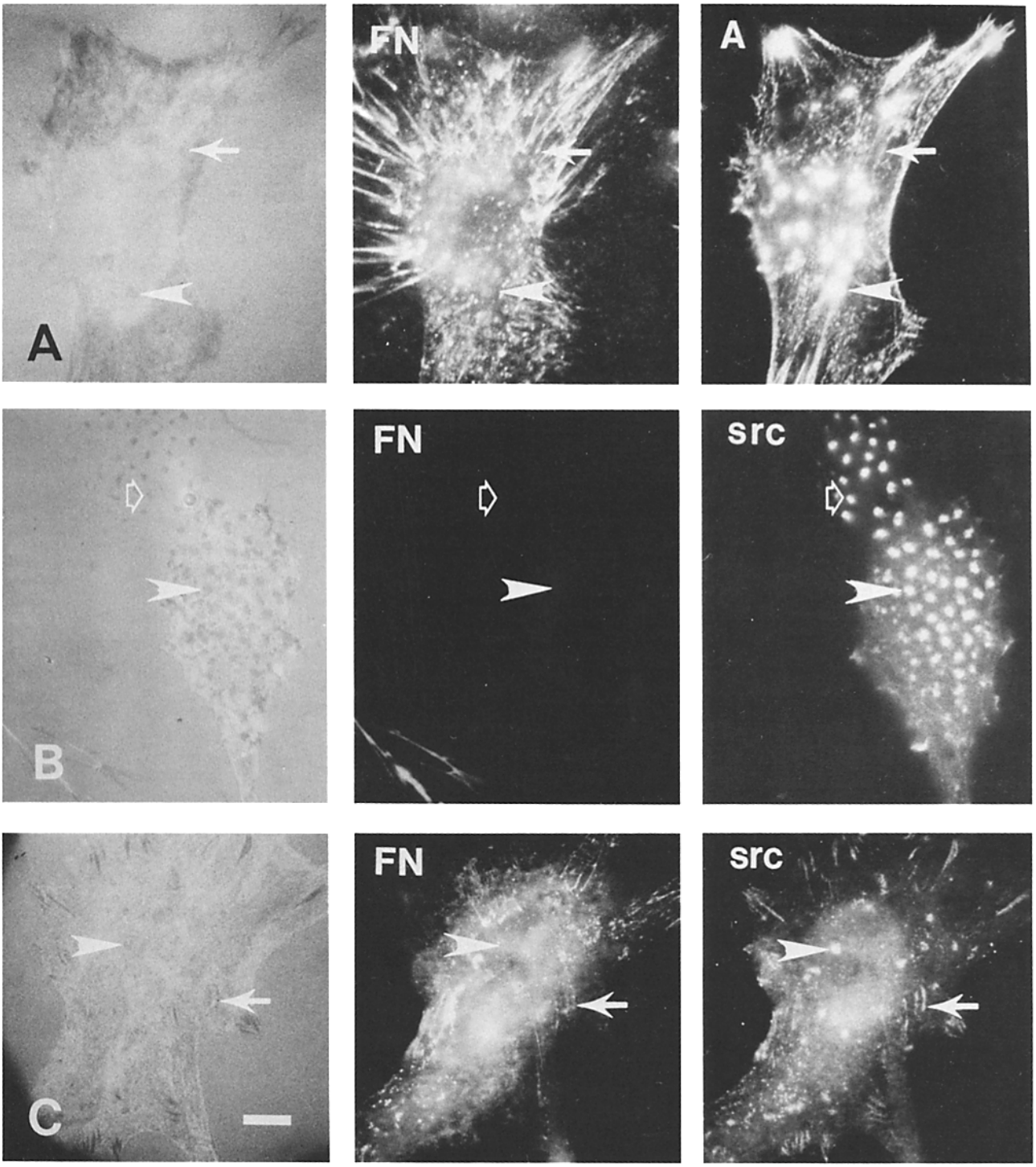

Figure 5. Visualization of alpha-actinin (*A*), fibronectin (*FN*), and RSV pp60^{src} (*src*) by double immunofluorescent labeling of RSV-CEF grown in the presence (rows *A* and *C*) and absence (row *B*) of added cellular fibronectin. The transformed cells were immunofluorescently double-labeled for pp60^{src}, A, and FN using EB7 monoclonal antibody, rabbit anti-alpha-actinin and goat anti-fibronectin antibodies, and also observed by IRM. Each row of panels (rows *A* and *C*) shows a typical fibronectin-reconstituted, transformed cell which simultaneously expressed RSV pp60^{src} and fibronectin cell surface linkage complexes. Arrows point to ECM contact sites in RSV-CEF with normal phenotypic morphology (with reconstituted fibronectin) and indicate linkage complexes at the cell–substratum interface, which are seen as fine positive- or negative-contrast IRM streaks and are labeled positively for FN, A, and pp60^{src}. Arrowheads point to rosette contacts under the centers of the cells that still remain in reconstituted cells showing otherwise normal phenotypic morphology. These contacts are seen as IRM spots and are labeled for RSV pp60^{src} and A, but not FN. Row *B* shows a transformed cell in the absence of added fibronectin which contains extensive RSV pp60^{src}, but lacks cell surface fibronectin. Arrowheads point to rosette contact sites under the center of the cell, while open arrows indicate the extended area of rosettes at the cell periphery. Bar, 10 μm.

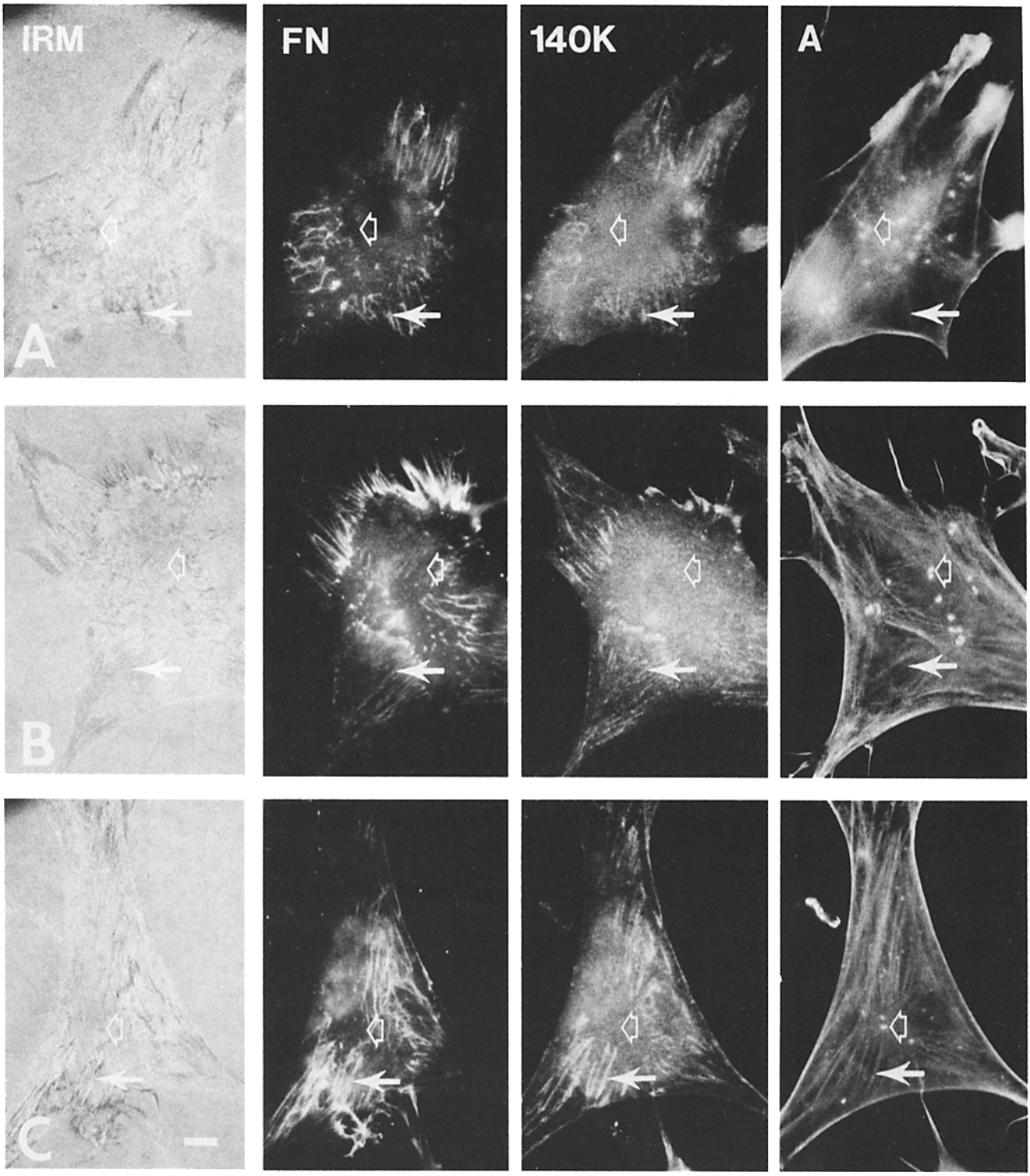

Figure 6. Distribution of actin (*A*), 140K receptor (*140K*), and fibronectin (*FN*) in RSV-CEF grown in the presence of added cellular fibronectin. The transformed, reconstituted cells were immunofluorescently triple-labeled for A, 140K, and FN using anti-140K JG22E monoclonal antibody, rabbit anti-actin and goat anti-fibronectin antibodies, and also observed by IRM. Each row of panels (*A–C*) shows a typical fibronectin-reconstituted, transformed cell, which simultaneously exhibited ECM contact sites at the cell periphery and rosette contact sites under the center of the cells. Arrows point to the same ECM contact sites in RSV-CEF with normal phenotypic morphology (with reconstituted fibronectin) and indicate linkage complexes at the cell–substratum interface, which are seen as fine IRM streaks and are labeled positively for A, 140K, and FN. Open arrows point to the same rosette contacts under the centers of the cells, which still remain in these cells that show otherwise normal phenotypic morphology; these contacts are seen as IRM spots and are labeled positively for A and only diffusely for 140K, but negatively for FN. Bar, 10 μm.

Table I. Concentration of 140K Antigen in Cell Layers and Culture Media of CEF and RSV-CEF

Samples*	μg/mg Protein‡			
	Cell layers	Medium	Total 140K	% 140K in medium
Confluent cultures				
CEF	7.34 ± 0.64	0.52 ± 0.07	7.86 ± 0.68	6.6 ± 0.7
RSV-CEF	6.74 ± 0.64	0.80 ± 0.14	7.54 ± 0.76	10.6 ± 0.9
Heavily confluent cultures				
CEF	7.29 ± 0.12	0.49 ± 0.11	7.78 ± 0.02	6.3 ± 1.4
RSV-CEF	6.63 ± 0.22	0.69 ± 0.06	7.32 ± 0.17	9.5 ± 1.0

* Samples consisted of second-passage cultures in 35-mm plates cultured for 2 d. Mock cultures containing only filtered culture media (containing 10% fetal bovine serum) were similarly incubated for 2 d and found to be negative in this assay.
‡ Concentration of the 140K antigen per mg total cell layer protein was measured by dot immunoblots using rabbit anti-140K antibodies. Values represent mean ± SD of triplicate determinations from independent cultures. The quantities and the percentages of total 140K released into medium were both statistically significantly higher for the RSV-transformed cells at both cell densities ($P < 0.05$).

at the cell periphery (Fig. 5 *C*). Alpha-actinin, but not fibronectin, was still found in these residual rosettes (Fig. 5 *A*). Quantitative immunofluorescence showed that these fibronectin-reconstituted cells exhibited not only increased levels of 140K staining at newly restored ECM contacts (see below), but also high levels of RSV pp60^{src} labeling at rosettes (Table II). The small proportion of cells that were representative of untransformed cells showed negligible RSV pp60^{src} labeling. These results established that the fibronectin-reconstituted cells we examined were indeed derived from RSV-transformed cells.

The addition of exogenous fibronectin to RSV-CEF cell layers also resulted in a striking reappearance of ECM contacts at the cell periphery and of fibronectin–140K cell surface linkage complexes, while more central regions of the transformed cells were relatively unaffected (Figs. 5 and 6). These linkage complexes appeared indistinguishable from those present in untransformed CEF, and they contained regions of codistribution of fibronectin, 140K complex, alpha-actinin, or actin (Figs. 5 and 6). The rosette contacts, though reduced in total area under the center of RSV-CEF, remained even after the addition of cellular fibronectin, and fibronectin and 140K complex were not localized to these contacts (Fig. 6). Thus, exogenous fibronectin can reconstitute fibronectin–140K–actin complexes at the cell periphery of transformed cells, but more central regions containing rosette contacts remain somewhat abnormal.

Table II. Immunofluorescent Morphometry of the Local Content of 140K Complex and Viral pp60^{src} in Normal and Transformed Cells

Structures	pp60^{src}*	140K‡	Control§
ECM contacts			
CEF‖	1	12	1
ts68-CEF, 41°C	3	10	1
RSV-CEF + cFN	3	9	1
Rosette contacts			
RSV-CEF	10	8	1
ts68-CEF, 37°C	6	6	1
RSV-CEF + cFN	6	6	1

* This column entitled pp60^{src} indicates the relative immunofluorescent intensity of antibody binding to the RSV transforming gene product, viral pp60^{src}, in cell contact sites of various cells using the mouse EB7 monoclonal antibody.
‡ This column entitled 140K indicates the relative immunofluorescent intensity of antibody binding to the 140K fibronectin receptor complex in cell contact sites of various cells using the mouse JG22E monoclonal antibody.
§ Immunofluorescent labeling of control mouse myeloma IgG, showing very low levels of nonspecific staining, is defined as one unit.
‖ Abbreviations used in this table: CEF, chick embryonic fibroblasts; ts68-CEF, 41°C, ts68-infected CEF grown at the temperature nonpermissive for transformation (41°C); RSV-CEF + cFN, RSV-CEF with reconstituted chick cellular fibronectin on the cell surface; ts68-CEF, 37°C, ts68-infected CEF grown at the temperature permissive for transformation (37°C).

Loss of 140K–Fibronectin Association on the Cell Surface after GRGDS Treatment

Treatment of cell cultures by the synthetic peptide GRGDS, which is derived from the sequence of a cell binding domain of fibronectin, inhibited the adhesion of cells to fibronectin substrata. These GRGDS effects on detachment of CEF from their fibronectin substrata and on cell surface linkage complexes were time-dependent (Fig. 7). In cells treated briefly with GRGDS (10 min), the 140K complex–fibronectin association was progressively lost at the cell periphery where the cells made new contacts with the substratum (Fig. 7), whereas the association temporarily remained intact at more centrally located, pre-existing cell-substratum attachment sites (the ECM contacts). Longer-term treatment (30 min) resulted in a complete detachment of cells, accompanied by the appearance of a diffuse pattern of 140K protein localization on the cells and of residual 140K-containing fibronectin fibers (probably representative of ripped membrane fragments) left behind on the substratum (Fig. 7), suggesting the existence of strong adhesive interactions at some of the preexisting cell surface linkage complexes that could not be completely reversed during GRGDS-induced cell detachment. It should be noted that the peptide treatment did not appear to affect most substratum-bound fibronectin fibrils,

Figure 7. Disruption of 140K association with linkage complexes during detachment of CEF from their substrata by GRGDS treatment of cells for 10 min (*top*), 20 min (*middle*), and 30 min (*bottom*). The association between 140K antigen and fibronectin (*FN*) was retained at certain pre-existing cell–substratum attachment sites near the centers of the cells (*narrow arrows*). Wide arrows indicate the absence of 140K-fibronectin associations at the cell periphery, even though the same residual fibronectin-containing fibers remain attached to the glass surface. The bright staining in the lower panels represents localization on the rounded cell body. Bar, 10 μm.

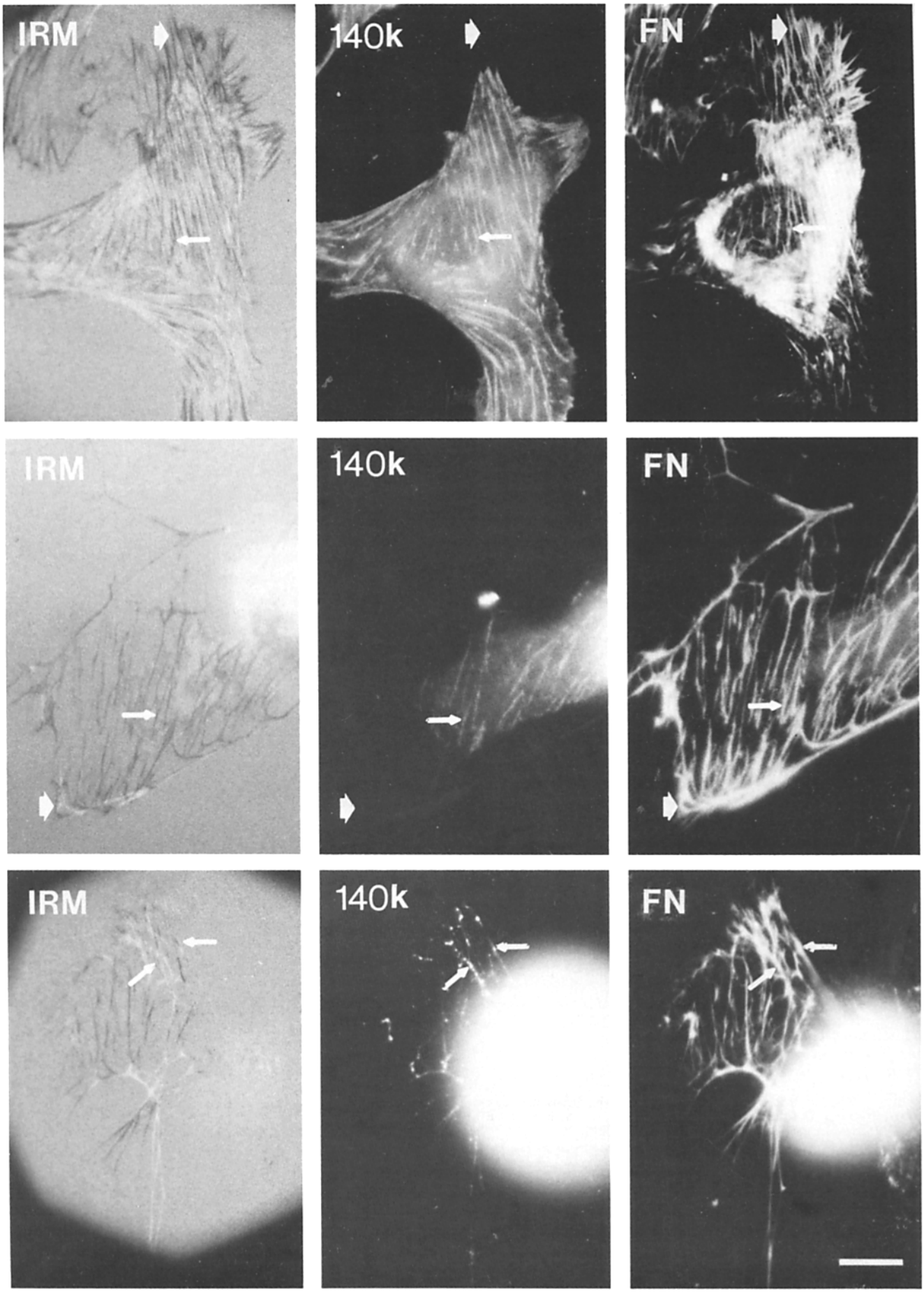
IRM
140k
FN
IRM
140k
FN
IRM
140k
FN

which remained in place after the cells had detached (Fig. 7), as might be expected for an agent that disrupts receptor–fibronectin binding rather than fibronectin–substratum binding.

Discussion

Fibronectin and its receptor complex of three membrane glycoproteins (the 140K complex) are spatially associated with microfilaments to form cell surface linkage complexes, which are thought to be involved in adhesive interactions between normal fibroblasts and their substrata (10, 11, 14). Such adhesive interactions occur at restricted regions of the plasma membrane, such as at close contact and ECM contact sites (11, 13). In the present studies, we have examined the regulation of such cell surface complexes comprised of extracellular, plasma membrane, and intracellular cytoskeletal elements. Our major findings are: (*a*) transformation disrupts the organization of cell surface linkage complexes normally present at ECM contact sites of untransformed fibroblasts; (*b*) in contrast, transformation has little effect on the total expression of the 140K fibronectin receptor complex itself, although surprisingly large proportions of the total can be released into the culture medium by transformed cells; (*c*) linear arrays of fibronectin–140K complex can be reconstituted on the transformed cell surface by the exogenous addition of purified cellular fibronectin to RSV-CEF; and (*d*) disruption of fibronectin–receptor interactions by a competitive synthetic peptide inhibitor mimics transformation in disrupting fibronectin–140K cell surface linkage complexes, even though pre-existing fibronectin fibrils remain in place on the substratum.

Our results suggest that cell surface fibronectin can regulate the distribution of its own receptor on the plasma membrane. The loss of fibronectin after transformation is accompanied by a loss of fibronectin–140K–alpha-actinin complexes. Culturing of transformed CEF in the presence of added cellular fibronectin has previously been shown to change the morphology of these cells toward that of normal cells and to restore a cell surface matrix of fibronectin (2, 40, 44). Such binding of exogenous cellular fibronectin to the transformed cell surface stimulates the reconstitution of fibronectin–140K linkage complexes (Fig. 5), demonstrating a regulatory role for fibronectin in that process. Our results also suggest that, once formed, fibronectin–140K complexes are relatively stable over short time periods. However, cells continue to form new complexes. In the presence of GRGDS, the adhesion of cells to fibronectin substrata is inhibited (23, 43), the formation of new fibronectin–140K linkage complexes is blocked (Fig. 7), and the cells ultimately detach. This finding again indicates a regulatory role for fibronectin–receptor interactions in regulating the localization of the 140K receptor at adhesive contact sites in the membrane, specifically in ECM contact sites.

In vivo localization studies are consistent with such a regulatory role for fibronectin in controlling the distribution of its receptor. In early developing smooth muscle and mesenchymal cells and during the angiogenic invasion of capillaries into lung mesenchyme, 140K antigens expressed on the cell surface of embryonic lung cells are redistributed from an initially uniform pattern to a punctate distribution co-localizing with fibronectin (8). In cultured fibroblasts, 140K antigens are distributed equally between the dorsal and ventral surfaces shortly after plating, but as cell spreading proceeds, they appear to become concentrated on the ventral surface in contact with fibronectin (11). In highly motile neural crest and somitic cells, 140K molecules are diffusely organized on the cell surface (16), while in nonmotile cells 140K molecules tend to be immobilized in well-defined areas of the cell surface close to fibronectin fibers; the architecture of the fibronectin fibers and their association with the cell membrane and with the cytoskeleton appears to be highly ordered and stable (10, 14, 16). Such multivalent fibrillar structures containing fibronectin may organize 140K fibronectin receptors on the cell surface, providing strong sites for the anchorage of cells to the ECM.

Conversely, rapid detachment of cell processes from fibronectin fibers may be favored by reversible binding of low-affinity cell surface receptors to fibronectin (1, 16), especially if the receptors were diffusely organized or if the fibers were acted upon by fibronectin-degrading proteases (12). The formation of fibronectin fibril and 140K complexes in the central, rosette-containing regions of transformed cells are prevented even after the addition of exogenous fibronectin, consistent with previous evidence for rapid turnover of fibronectin at these sites (12). These mechanisms would avoid the establishment of stable 140K-containing linkage complexes, thus permitting rapid cell migration or invasion.

Although the ECM may direct gene expression in some systems (3), the total content of 140K molecules in RSV-transformed cells appears to be independent of quantities of fibronectin. Nearly normal amounts of 140K antigen are present in transformed cells lacking cell surface fibronectin, indicating a lack of coordinate regulation of this ligand–receptor pair. Additionally, during early embryonic development of lung cells, 140K appears before the accumulation of fibronectin and laminin on the cell surface (8), again suggesting independent regulation. Our results also strongly suggest that a loss of cell surface receptors for fibronectin in these transformed cells is not the reason for the lack of cell surface fibronectin, since we found that (*a*) the 140K complex is present in nearly normal quantities on the transformed cells, (*b*) added fibronectin can reconstitute the cell surface linkages in RSV-CEF, and (*c*) the attachment and spreading of RSV-CEF on fibronectin substrata was unimpaired (10). On the other hand, it is possible that the increased release of 140K complexes into culture medium of RSV-CEF might have modest effects on the capacity of the transformed cell surface to retain bound fibronectin (30).

After completion of the portion of our studies showing that fibronectin receptor organization was lost after transformation and its presentation in abstract form (37), Giancotti et al. (18) reported a similar loss of organization of a possibly related 135K glycoprotein in transformed mouse 3T3 fibroblasts. One puzzling and potentially interesting difference between the two studies was that their GP135 protein was located in adhesion plaques (focal contacts) of 3T3 cells, while we could not find localization of our 140K antigen at such sites in CEF.

In summary, our results support the idea that fibronectin can regulate the distribution of its own receptor. This type of externally controlled receptor system could provide a particularly sensitive mechanism for locally regulating the organization of intracellular cytoskeletal elements such as alpha-

actinin and microfilament bundles that may associate directly or indirectly with the fibronectin receptor. Such a system could rapidly re-adjust microfilament systems and cell polarity in response to the local extracellular microenvironment, for example, when a single cell simultaneously contacts a basement membrane, various extracellular matrices, and other cells.

We thank Mrs. Catherine Weinstock and Mrs. Yun-Yun Chen for technical assistance, and Dr. Jinq-May Chen and Dr. Susette Mueller for helpful discussions.

This investigation was supported by Public Health Service grant numbers R01-CA39077 and R01-HL33711 awarded by the National Institutes of Health, Department of Health and Human Services to W.-T. Chen.

Received for publication 12 March 1986, and in revised form 10 June 1986.

References

1. Akiyama, S. K., S. S. Yamada, and K. M. Yamada. 1986. Characterization of a 140kD avian cell surface antigen as a fibronectin-binding molecule. *J. Cell Biol.* 102:442–448.

2. Ali, I. U., V. M. Mautner, R. Lanza, and R. O. Hynes. 1977. Restoration of normal morphology, adhesion and cytoskeleton by addition of a transformation-sensitive surface protein. *Cell.* 11:115–126.

3. Bissell, M. J., H. G. Hall, and G. Parry. 1981. How does the extracellular matrix direct gene expression? *J. Theor. Biol.* 99:31–68.

4. Brackenbury, R., M. E. Greenberg, and G. M. Edelman. 1984. Phenotypic changes and loss of N-CAM-mediated adhesion in transformed embryonic chicken retinal cells. *J. Cell Biol.* 99:1944–1954.

5. Bronner-Fraser, M. E. 1985. Alterations in neural crest migration by a monoclonal antibody that affects cell adhesion. *J. Cell Biol.* 101:610–617.

6. Brown, P., and R. L. Juliano. 1985. Selective inhibition of fibronectin-mediated cell adhesion by monoclonal antibodies to a cell-surface glycoprotein. *Science (Wash. DC).* 228:1448–1451.

7. Burnette, W. N. 1981. "Western blotting": electrophoretic transfer of proteins from sodium dodecyl sulfate-polyacrylamide gels to unmodified nitrocellulose and radiographic detection with antibody and radiolabeled protein A. *Anal. Biochem.* 112:195–203.

8. Chen, W. T., J.-M. Chen, and S. C. Mueller. 1986. Coupled expression and colocalization of 140K cell adhesion molecules, fibronectin, and laminin during morphogenesis and cytodifferentiation of chick lung cells. *J. Cell Biol.* 103:1073–1090.

9. Chen, W.-T., J.-M. Chen, S. J. Parsons, and J. T. Parsons. 1985. Local degradation of fibronectin at sites of expression of the transforming gene product pp60^{src}. *Nature (Lond.).* 316:156–158.

10. Chen, W.-T., T. Hasegawa, E. Hasegawa, C. Weinstock, and K. M. Yamada. 1985. Development of cell surface linkage complexes in cultured fibroblasts. *J. Cell Biol.* 100:1103–1114.

11. Chen, W.-T., J. M. Greve, D. I. Gottlieb, and S. J. Singer. 1985. The immunocytochemical localization of 140 Kd cell adhesion molecules in cultured chicken fibroblasts, and in chicken smooth muscle and intestinal epithelial tissues. *J. Histochem. Cytochem.* 33:576–586.

12. Chen, W.-T., K. Olden, B. A. Bernard, and F. F. Chu. 1984. Expression of transformation-associated protease(s) that degrade fibronectin at cell contact sites. *J. Cell Biol.* 98:1546–1555.

13. Chen, W.-T., and S. J. Singer. 1982. Immunoelectron microscopic studies on the sites of cell-substratum and cell-cell contacts in cultured fibroblasts. *J. Cell Biol.* 95:205–222.

14. Damsky, C. H., K. A. Knudsen, D. Bradley, C. A. Buck, and A. F. Horwitz. 1985. Distribution of the CSAT cell-matrix adhesion antigen on myogenic and fibroblastic cells in culture. *J. Cell Biol.* 100:1528–1539.

15. David-Pfeuty, T., and S. J. Singer. 1980. Altered distributions of the cytoskeletal proteins vinculin and alpha-actinin in cultured fibroblasts transformed by Rous sarcoma virus. *Proc. Natl. Acad. Sci. USA.* 77:6687–6691.

16. Duband, J.-L., S. Rocher, W.-T. Chen, K. M. Yamada, and J. P. Thiery. 1986. Cell adhesion and migration in the early vertebrate embryo: location and possible role of the putative fibronectin receptor complex. *J. Cell Biol.* 102: 160–178.

17. Fairbairn, S., R. Gilbert, G. Ojakian, R. Schwimmer, and J. P. Quigley. 1985. The extracellular matrix of normal chick embryo fibroblasts: its effect on transformed chick fibroblasts and its proteolytic degradation by the transformants. *J. Cell Biol.* 101:1790–1798.

18. Giancotti, F. G., P. M. Comoglio, and G. Tarone. 1986. A 135,000 molecular weight plasma membrane glycoprotein involved in fibronectin-mediated cell adhesion. *Exp. Cell Res.* 163:47–62.

19. Greve, J. M., and D. I. Gottlieb. 1982. Monoclonal antibodies which alter the morphology of cultured chick myogenic cells. *J. Cell. Biochem.* 18:221–229.

20. Hasegawa, T., E. Hasegawa, W.-T. Chen, and K. M. Yamada. 1985. Characterization of a membrane glycoprotein complex implicated in cell adhesion to fibronectin. *J. Cell. Biochem.* 28:307–318.

21. Hayman, E. G., E. Engvall, and E. Ruoslahti. 1981. Concomitant loss of cell surface fibronectin and laminin from transformed rat kidney cells. *J. Cell Biol.* 88:353–357.

22. Hayman, E. G., A. Oldberg, G. R. Martin, and E. Ruoslahti. 1982. Codistribution of heparan sulfate proteoglycan, laminin, and fibronectin in the extracellular matrix of normal rat kidney cells and their coordinate absence in transformed cells. *J. Cell Biol.* 94:28–35.

23. Hayman, E. G., M. D. Pierschbacher, and E. Ruoslahti. 1985. Detachment of cells from culture substrate by soluble fibronectin peptides. *J. Cell Biol.* 100:1948–1954.

24. Horwitz, A., K. Duggan, R. Greggs, C. Decker, and C. Buck. 1985. The CSAT antigen has properties of a receptor for laminin and fibronectin. *J. Cell Biol.* 101:2134–2144.

25. Hynes, R. O., and A. Wyke. 1975. Alterations in surface proteins in chicken cells transformed by temperature-sensitive mutants of Rous sarcoma virus. *Virology.* 64:492–504.

26. Hynes, R. O., and K. M. Yamada. 1982. Fibronectins: multifunctional modular glycoproteins. *J. Cell Biol.* 95:369–377.

27. Jahn, J., W. Schiebler, and P. Greengard. 1984. A quantitative dot-immunobinding assay for proteins using nitrocellulose membrane filters. *Proc. Natl. Acad. Sci. USA.* 81:1684–1687.

28. McDonald, J. A. 1986. Roles of fibronectin in lung disease. *In* Fibronectin. D. F. Mosher, editor. Academic Press, Inc., New York. In press.

29. Neff, N. T., C. Lowrey, C. Decker, A. Tovar, C. Damsky, C. Buck, and A. F. Horwitz. 1982. A monoclonal antibody detaches embryonic skeletal muscle from extracellular matrices. *J. Cell Biol.* 95:654–666.

30. Olden, K., and K. M. Yamada. 1977. Mechanism of the decrease in the major cell surface protein of chick embryo fibroblasts after transformation. *Cell.* 11:957–969.

31. Parsons, S., D. McCarley, C. Ely, D. Benjamin, and J. T. Parsons. 1984. Monoclonal antibodies to Rous sarcoma virus pp60^{src} react with enzymatically active cellular pp60^{src} of avian and mammalian origin. *J. Virol.* 52:272–282.

32. Pytela, R., M. D. Pierschbacher, and E. Ruoslahti. 1985. Identification and isolation of a 140kd cell surface glycoprotein with properties expected of a fibronectin receptor. *Cell.* 40:191–198.

33. Rogalski, A. A., and S. J. Singer. 1985. An integral glycoprotein associated with the membrane attachment sites of actin microfilaments. *J. Cell Biol.* 101:785–801.

34. Ruoslahti, E. 1984. Fibronectin in cell adhesion and invasion. *Cancer Metastasis Rev.* 3:45–51.

35. Shriver, K., and L. Rohrschneider. 1981. Organization of pp60^{src} and selected cytoskeletal proteins within adhesion plaques and junctions of Rous sarcoma virus-transformed rat cells. *J. Cell Biol.* 89:525–535.

36. Trinkaus, J. P. 1984. Cells into Organs. The Forces that Shape the Embryo. 2nd ed. Prentice Hall, Inc., Englewood Cliffs, NJ. 543 pp.

37. Wang, J., C. Weinstock, T. Hasegawa, S. S. Yamada, K. M. Yamada, and W.-T. Chen. 1985. Altered organization of 140Kd putative ECM receptors in fibroblasts transformed by Rous sarcoma virus or treated with fibronectin cell-binding peptides. *J. Cell Biol.* 101(5, Pt. 2):332a. (Abstr.).

38. Weber, M. J., A. H. Hale, and L. Losasso. 1977. Decreased adherence to the substrate in Rous sarcoma virus-transformed chicken embryo fibroblasts. *Cell.* 10:45–51.

39. Willingham, M. C., K. M. Yamada, S. S. Yamada, J. Pouyssegur, and I. Pastan. 1977. Microfilament bundles and cell shape are related to adhesiveness to substratum and are dissociable from growth control in cultured fibroblasts. *Cell.* 10:375–380.

40. Yamada, K. M. 1978. Immunological characterization of a major transformation-sensitive fibroblast cell surface glycoprotein: localization, redistribution, and role in cell shape. *J. Cell Biol.* 78:520–541.

41. Yamada, K. M., S. K. Akiyama, T. Hasegawa, E. Hasegawa, M. J. Humphries, D. W. Kennedy, K. Nagata, H. Urushihara, K. Olden, and W.-T. Chen. 1985. Recent advances in research on fibronectin and other cell attachment proteins. *J. Cell. Biochem.* 28:79–97.

42. Yamada, K. M., and D. W. Kennedy. 1984. Dualistic nature of adhesive protein function: fibronectin and its biologically active peptide fragments can auto-inhibit fibronectin function. *J. Cell Biol.* 98:29–36.

43. Yamada, K. M., and D. W. Kennedy. 1985. Amino acid sequence specificities of an adhesive recognition signal. *J. Cell. Biochem.* 28:77–98.

44. Yamada, K. M., S. S. Yamada, and I. Pastan. 1976. Cell surface protein partially restores morphology, adhesiveness, and contact inhibition of movement to transformed fibroblasts. *Proc. Natl. Acad. Sci. USA.* 73:1217–1221.